LAB EX 4 TOP

XL-W Xlerator Hand Dryer Flow Analysis
AME 20213: Measurements and Data Analysis

~~December 10, 2009~~
(Began with kit 5) ✓

Abstract

This paper presents a field study of the output flow of the XL-W Xlerator hand dryer in the second floor LaFortune men's bathroom. A pitot static tube and Portable Setra Pressure Transducer measurement system to be used to measure the flow was calibrated using a wind tunnel and a Model 239 Setra pressure transducer. The calibration data also determined that hysteresis would not have a significant effect on data measured by the pitot static measurement system. Also to minimize the error, the effect of yaw angle on this pitot static measurement system was analyzed for angles from 0 to 30 degrees and it was determined that yaw angle has little effect when the pitot probe was kept at angles of less than 5 degrees with the flow.

Once the measurement system was calibrated and determined to be suitable for the field study, it was used to map the flow of the hand dryer output over a Cartesian grid. A two dimensional numerical approximation was used over the Cartesian grid, and the volumetric flow rate was calculated to be 12.78 ± 0.10 ft^3/min (95%). The volumetric flow rate was then used to calculate the mass flow rate which was 0.026 ± 0.070 slug/min (95%). Using these values and the area of the flow, the mean velocity was calculated as $3{,}284 \pm 3.6$ ft/min (95%). Then using a K-type Thermocouple measurement system, the temperature of the hand dryer flow was measured as 597 ± 13 °R (95%). The values of the mean velocity and the temperature of the hand dryer flow were compared to the manufacturer specifications and it was found that the measured mean velocity was 78.8% less than the listed theoretical velocity and the measured temperature was 0.3% different than the listed temperature. These findings led to the conclusion that the hand dryer was running at a lower operational power setting.

Contents

Figures

Tables

1 Nomenclature

English

A	Cross-sectional area (ft^2)
L	Length (in)
m	Number of rows of points in Cartesian grid
$\dot{m}$	Mass flow rate (slug/min)
n	Number of columns of points in Cartesian grid
p	Pressure (lb/ft^2)
Q	Volumetric flow rate (ft^3/min)
Re	Reynolds number (Dimensionless)
R	Ideal Gas Constant (ft-lb/slug-°R)
S	Rectangle
T	Temperature (°R)
v	Velocity (ft/min)
$\overline{v}$	Mean velocity (ft/min)
x	Horizontal Displacement (ft)
y	Vertical Displacement (ft)

Greek

μ	Dynamic viscosity (slug/ft-s)
ρ	Density ($slug/ft^3$)
Δ	Change in

Subscripts

char	characteristic
cr	critical
i	index
j	index
o	stagnation point

2 Introduction

The purpose of this laboratory experiment was to measure the mean velocity, volumetric flow rate, and mass flow rate of the XL-W Xlerator hand dryer in the LaFortune second floor men's bathroom and compare these parameters to the manufacturer specifications. As is well known, the idea of a hand dyer is to produce a heated flow of air over a person's hands. The Xlerator manufacturer specification lists the air velocity produced by the hand dryer to be 16,000 ft/min at the outlet and 14,000 ft/min at the hands[1]. However, what are not well known are the actual parameters of the flow that the hand dryer outputs while in use. Thus, this field test was conducted in order to produce measured parameters of the flow generated by a hand dryer in use, which could be compared to the manufacturer's listed specifications.

To measure parameters of a flow, it was first necessary to understand the characteristics of the flow being studied. One of the most important aspects of a fluid dynamics problem is determining whether the flow is laminar or turbulent. In this respect, the Reynolds number is an important characteristic to understand. Fundamentally, the Reynolds number measures the ratio of inertial forces to viscous forces, but more importantly, the value of the critical Reynolds number determines the location of where a flow transitions from laminar to turbulent. For this problem, we are interested in the air flow beneath the outlet of the hand dryer; therefore, the flow was considered a 'free stream flow.' For free stream flows, the critical Reynolds number is assumed to be approximately 10^5 [2]. The distance at which the flow becomes unstable is called the characteristic length and is calculated by manipulating the Reynolds number equation as seen in equation [1].

$$L_{char} = \frac{\mathrm{Re}_{cr}\,\mu}{\rho v}. \qquad [1]$$

In this equation, L_{char} is the characteristic length, Re_{cr} is the critical Reynolds number, μ is the dynamic viscosity of the fluid, v is the velocity of the flow, and ρ is the density of the fluid which is a function of temperature and pressure. The density is calculated using a modified form of the ideal gas law which is given in equation [2] where R is the ideal gas constant, T is the temperature of the fluid, and p is the absolute pressure of the flow.

$$\rho = \frac{p}{RT} \qquad [2]$$

For the hand dryer free stream flow, the characteristic length is the distance downstream of the outlet at which the flow becomes turbulent. The measurements of the flow were focused on the laminar region; therefore, the characteristic length was an important value to be determined. The rationale for taking measurements in the laminar region is that in the laminar region, a flow can be approximated as a steady streamline, which is important when measuring the velocity of a flow.

Historically, pitot static probes have been a reliable instrument when it comes to measuring the velocity of a free stream flow. The theory behind the function of a pitot static probe is well understood. On a pitot static probe, there are two inlets. One inlet faces the free stream flow while the other inlet is perpendicular to the flow (Figure 1). By facing the free stream, the first inlet corresponds to the total pressure of the flow, while the second, perpendicular, inlet corresponds to the static pressure. At the opposite end of the pitot tube, a

separate port for each inlet is connected to a pressure transducer. The total pressure from the first inlet is fed to one plenum while the static pressure from the other is fed to a second plenum. The pressure difference between the two inlets causes the plenums to come closer together. A capacitive sensor between the two plenums converts this change in distance into a voltage output when coupled with a capacitance Wheatstone bridge. This voltage output can then be displayed and stored by a data acquisition system. At this point, this measurement system has only measured the difference between the static and the dynamic pressures. In order to obtain information about the velocity of the flow, the Bernoulli equation must be applied.

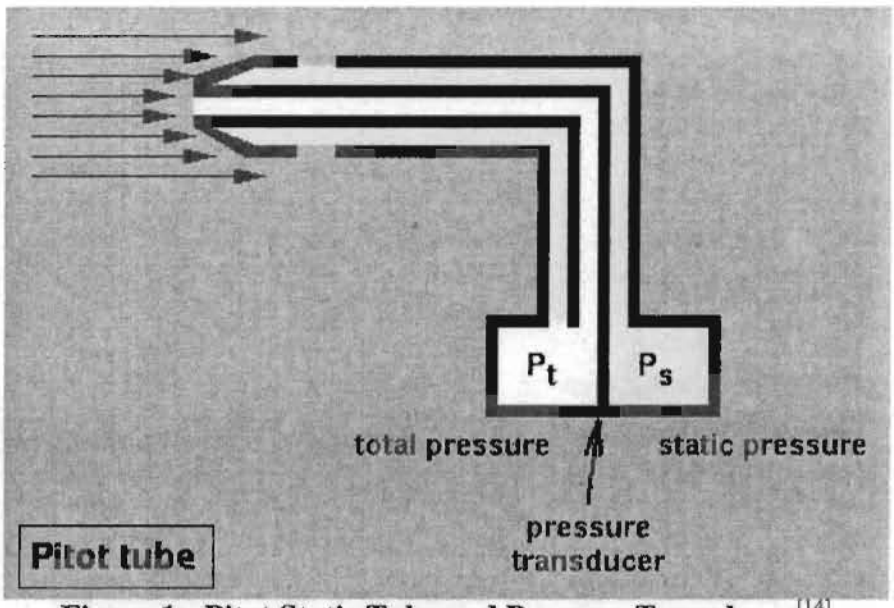

Figure 1: Pitot Static Tube and Pressure Transducer[14]

The Bernoulli equation represents an essential relationship between the pressure difference and velocity of a flow. To apply the Bernoulli equation, certain assumptions must be made. The flow in question must be steady, incompressible, irrotational, frictionless, and along the same streamline. If all are true, the Bernoulli equation can be considered valid for the flow being studied. The Bernoulli equation is defined as,

$$p_o + \rho\frac{v_o^2}{2} = p + \rho\frac{v^2}{2}, \qquad [3]$$

where p_o is the total pressure, p is the static pressure, v_o is the velocity at the stagnation point, ρ is the density of the fluid, and v is the fluid flow velocity[3]. At the stagnation point, v_o is equal to zero, therefore the Bernoulli equation reduces to

$$v = \sqrt{\frac{2\Delta p}{\rho}}, \qquad [4]$$

where Δp is the difference between the total pressure and the static pressure (p_o-p) and ρ is the temperature dependent density of the fluid. From the pitot static tube, the difference between the static pressure and the dynamic pressure is known. Substituting this pressure difference into the

reduced Bernoulli equation yields the velocity of the free stream flow to which the pitot tube is subjected.

However, the Bernoulli equation requires a temperature dependent fluid density. To measure the temperature of the flow, a thermocouple measurement system is used. A thermocouple measurement system consists of a thermocouple, a bridge/amplifier, and a data acquisition system. The thermocouple outputs a voltage which can be converted into a temperature that can be used to determine the density of the fluid.

Once the velocity of the fluid is known, the volumetric and mass flow rates can be calculated for the flow as a whole. The volumetric flow rate is defined as

$$Q = \overline{v}A = \int_A v dA\,, \qquad [5]$$

where Q is the volumetric flow rate, $\overline{v}$ is the mean velocity, v is the velocity, and A is the cross-sectional area of the flow. Since the velocity is modeled as points of a Cartesian grid (See Appendix A Figure 1) the volumetric flow rate definition must be modified. This results in equation [6],

$$Q = \int_a^b \int_c^d v dy dx\,, \qquad [6]$$

over the rectangle $S = \{(x,y) : a \le x \le b,\ c \le y \le d\}$. To approximate this integral, a numerical scheme is applied. This numerical scheme approximates the integral by estimating the volume under the surface of the function. The Simpson's Rule was preferred over the Trapezoidal Rule since the order of error is much less. The Simpson's Rule, which requires an even number of points, is given by equation [7] [4],

$$\begin{aligned}
\int_S f(x,y)dA &= \int_a^b \int_c^d v(x,y)dydx \\
&\approx \frac{1}{9}\Delta x \Delta y [v(a,c)+v(a,d)+v(b,c)+v(b,d) \\
&+4\sum_{j=1}^{(n+1)/2} v(a,y_{2j-1}) + 2\sum_{j=1}^{(n-1)/2} v(a,y_{2j}) \\
&+4\sum_{j=1}^{(n+1)/2} v(b,y_{2j-1}) + 2\sum_{j=1}^{(n-1)/2} v(b,y_{2j}) \\
&+4\sum_{i=1}^{(m+1)/2} v(x_{2i-1},c) + 2\sum_{i=1}^{(m-1)/2} v(x_{2i},c) \\
&+4\sum_{i=1}^{(m+1)/2} v(x_{2i-1},d) + 2\sum_{i=1}^{(m-1)/2} v(x_{2i},d) \\
&+16\sum_{j=1}^{(n+1)/2}\left(\sum_{i=1}^{(m+1)/2} v(x_{2i-1},y_{2j-1})\right) + 8\sum_{j=1}^{(n-1)/2}\left(\sum_{i=1}^{(m+1)/2} v(x_{2i-1},y_{2j})\right) \\
&+8\sum_{j=1}^{(n+1)/2}\left(\sum_{i=1}^{(m-1)/2} v(x_{2i},y_{2j-1})\right) + 4\sum_{j=1}^{(n-1)/2}\left(\sum_{i=1}^{(m-1)/2} v(x_{2i},y_{2j})\right)], \qquad [7]
\end{aligned}$$

where Δx is the change in the horizontal direction, Δy is the change in the vertical direction, and

$$x_i = a + i\Delta x \qquad i = \{0,1,...,m\}$$
$$y_j = c + j\Delta y \qquad j = \{0,1,...,n\}.$$

After the Simpson's Rule is applied, the volumetric flow rate is known. Next, to calculate the mass flow rate, $\dot{m}$, equation [8] is used, where ρ is the density of the fluid, $\overline{v}$ is the mean velocity, and A is the cross-sectional area of the flow.

$$\dot{m} = \rho \overline{v} A = \int_a^b \int_c^d \rho v(x,y)\,dx\,dy \qquad [8]$$

Due to the initial assumption of incompressibility, the mass flow rate can be calculated assuming the density to be constant throughout the flow. Therefore the mass flow rate can be calculated by multiplying the density by the result of equation [7]. After the volumetric flow rate and mass flow rate have been calculated, a relation between equation [5] and equation [6] can be formulated and solved for the mean velocity as shown in equation [9].

$$\overline{v} = \frac{\int_A v\,dA}{A} = \frac{\int_a^b \int_c^d v(x,y)\,dx\,dy}{(b-a)(d-c)} \qquad [9]$$

3 Experimental Approach and Procedure

3.1 Calibration Approach

3.1.1 Pressure Transducer

Before an accurate measurement could be obtained in the field, the Portable Setra pressure transducer (PT) used to convert the pitot tube pressure difference into voltage was calibrated. The Setra PT was calibrated against a Model 239 Setra pressure transducer that was specifically designed for low pressure applications that require high accuracy[5] [6]. A pitot static tube was fixed in a low speed wind tunnel, located in the Engineering Learning Center, with a pressure take-off "T" for static pressure and another for total pressure. One pair of pressure take-offs was connected to the Model 239 and the other pair was connected to the Portable Setra PT. The Model 239 Setra pressure transducer was linked directly to a computer and output a single pressure difference stored in Labview. The Portable Setra PT fed voltages to a LabQuest data acquisition system (DAQ) which recorded 500 Hz for 2 seconds per run.

In order to obtain an accurate calibration, various scenarios were accounted for during the calibration procedure. The wind tunnel was run with no flow to acquire a zero voltage and pressure difference to correct for any noise in the wind tunnel. The first data set was gathered for velocities ranging from 10% to 100% and back to 10% power using increments of 10%, but were obtained through a Teaching Assistant. Only the points of increasing power were used to

create the calibration curve. The relationship between pressure difference and voltage was assumed to be linear and the method of least squares fit was used to create the calibration equation[7]. The points decreasing from 100% power were collected to demonstrate the effects of hysteresis (See Appendix B: MATLAB code). The next four data sets were assembled from kit 5 with the purpose of accounting for the effect of yaw angle. The four data sets were collected for velocities ranging from 20% to 100% by increments of 20% with the pitot tube at angles of 5, 10, 15, and 30 degrees with the flow (See Appendix C: MATLAB code).

3.1.2 Thermocouple

The thermocouple measurement system used to measure the temperature of the flow was composed of a K-type thermocouple, thermocouple module, and the LabQuest DAQ[8] [9]. Before the thermocouple was turned on, the LabQuest was zeroed to eliminate an initial voltage reading. When the thermocouple was turned on, the voltage on the LabQuest DAQ was sampled at 500 Hz for 2 seconds in the Learning Center. Then this voltage was compared to the room temperature obtained from a thermometer and the y-intercept of the calibration curve was calculated using a given sensitivity (See Appendix B: MATLAB code).

3.2 Experimental Set Up

The field experiment was conducted in the second floor LaFortune bathroom using the XL-W Xlerator after calibration data had been acquired. Before the pitot tube measurement system was assembled, a temperature measurement was taken of the hand dryer flow. Using this temperature, the characteristic length was determined from equation [1]. Next, the pitot tube measurement system was assembled with a cart, a cardboard box, two rectangular recycling bin lids and a ruler/level onto which the pitot tube was clamped (Figure 2). This assortment of items brought the height of the pitot tube well within the characteristic length, but not inside the outlet. The ruler resting on the recycling bins created a stable shelf that kept the pitot tube level. To stabilize the pitot tube, the cart was attached to the sink with Scotch packing tape. At both ends of the rectangular recycling bin, a paper ruler with a 1/16 inch scale was taped down and lined up to ensure that the ruler/level stayed perpendicular to the wall. These rulers also accounted for changes in the x direction. A paper ruler with a 1/16 inch scale was taped to the ruler/level to quantify shifts of the pitot tube in the y direction. In order to maximize the number of points, minimize the distance between points, and represent the entire cross-sectional flow, an 8x8 grid was created that covered the entire back half of the hand dryer outlet tube (See Appendix A Figure 1). Symmetry was assumed across the center line allowing the entire flow to be modeled. Since the size of the outlet was measured at 7/8 inch, the horizontal increment was 1/8 inch and the vertical increment was 1/16 inch. The pitot tube was connected to the Portable Setra PT and, in turn, was connected to the LabQuest DAQ. For all 64 points, the flow was sampled at 500 Hz for 3 seconds. To eliminate any effects of hysteresis, the hand dryer was turned on for 5 seconds before any data was collected.

great

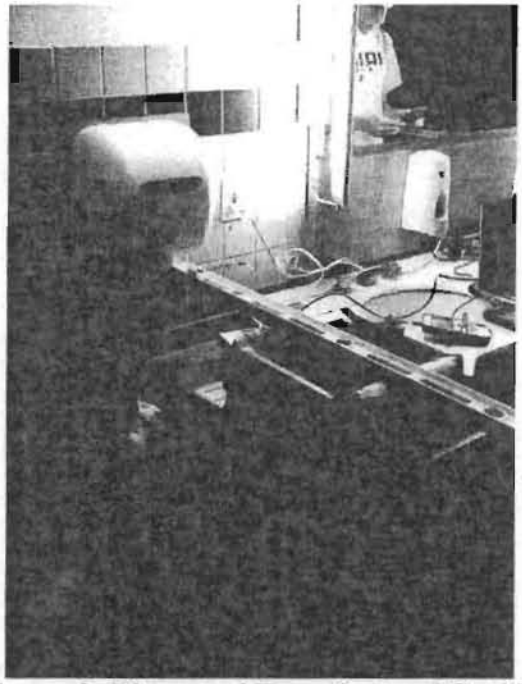

nice setup!

Figure 2: Picture of Experimental Set Up

3.3 Uncertainty

There are many sources of uncertainty inherent of the testing process. Some of these errors are a result of systematic errors related to accuracy while others are random errors due to repeatability. Table 1 lists the quantification of the error in each parameter and the origin of each error. All calculations of error in this study use a large scale approximation with 95% confidence.

Table 1: Parameters for Which Uncertainty Was Calculated

Parameter	Units	Measured or Calculated	Estimated Uncertainty (95% Confindence)
Calibration Bounds	V	Calculated	± 0.028 V
Pressure Uncertainty (xerror)	in H_2O	Measured	± 0.0012 in H_2O
Voltage Uncertainty (yerror)	V	Measured	± 0.20 V
Hysteresis Uncertainty	V	Calculated	± 0.032 V
Thermocouple Uncertainty	°R	Measured	± 13 °R
Barometric Pressure Uncertainty	lb/ft^2	Measured	± 0.71 lb/ft^2
Density Uncertainty	$slug/ft^3$	Calculated	± $4.6*10^{-5}$ $slug/ft^3$
Mean Voltage Uncertainty	V	Measured	± 0.20 V
Mean Pressure Uncertainty	lb/ft^2	Calculated	± 0.14 lb/ft^2
Mean Velocity Uncertainty	ft/min	Calculated	± 3.6 ft/min
Increment Uncertainty	ft	Measured	± 0.0026 ft
Volumetric Flow Rate Uncertainty	ft^3/min	Calculated	± 0.10 ft^3/min
Mass Flow Rate Uncertainty	slug/min	Calculated	± 0.070 slug/min
Characteristic Length Uncertainty	in	Calculated	± 0.0017 in

In the calculation of the calibration uncertainty bounds, a precision interval is used with the standard error of fit. This standard error of fit is multiplied by a Student's t variable using 95% confidence[10]. The horizontal error bars are a result of a large scale approximation of an instrument error of 0.14% of the full scale range and a resolution error of the Model 239 Setra pressure transducer[6]. The error in the voltage reading result in the vertical error bars of the calibration. A large scale approximation of the DAQ resolution error, instrument error, and the Portable Setra PT full scale range error of 1% combined in quadrature is taken[5] [11]. It is worth noting that the Portable Setra PT instrument error overshadows all other errors. Hysteresis introduces an elemental uncertainty in predicting the output of the calibration equation at a point in time because the current state of the flow cannot be known without information about the history of the flow leading up to that point. The hysteresis uncertainty in the calibration represents the largest difference between the calibration line and measured voltage.

Density is calculated as a function of the barometric pressure and temperature of a fluid. A thermocouple measurement system was used to find the temperature[12]. The instrument errors of the K-type thermocouple and thermocouple module were combined in quadrature with the resolution error and a type 2 uncertainty computed from the mean temperature sampled by the thermocouple[8] [9]. The barometric pressure uncertainty only depends on the resolution of the barometer. The thermocouple and barometric uncertainties were used in the uncertainty formation of equation [2] to calculate the uncertainty in density.

There was also an impact of uncertainty on the hand dryer measurements. The uncertainty of the mean voltages stored in the LabQuest DAQ were found by adding in quadrature the calibration voltage uncertainty to the type 2 uncertainty computed from the mean voltage sampled by the LabQuest DAQ. As with the calibration voltage uncertainty, the mean voltage uncertainty is dominated by the full scale range error of the Portable Setra PT[5]. These voltage uncertainties were averaged and converted to a pressure uncertainty. Then another type 2 uncertainty was computed to find the mean pressure uncertainty. This mean pressure uncertainty was applied to equation [9] along with the density uncertainty and a mean velocity uncertainty was calculated. To be able to calculate the uncertainty in the volumetric and mass flow rate, first the increment uncertainty had to be calculated. The x and y increment uncertainties were found using the resolution error of the ruler. The volumetric flow rate and mass flow rate errors were discovered using equations [5] and [8] for uncertainty. There was also an error due to the application of the Simpson's Rule[4]. This error is 4th order and described as equaling the sum of the order of the x increment to the fourth power and the y increment to the fourth power. The characteristic length uncertainty was calculated using equation [1]. This uncertainty was important because a distance within bounds of the characteristic length uncertainty could result in measurements taken in turbulent flow. All uncertainty calculations are located in Appendix D.

4 Results

4.1 Calibration Results and Initial Calculations

Using the method of least squares for the wind tunnel data for increasing power only, a calibration curve was determined with a sensitivity of 9.919 V/in-H_2O and a coefficient of determination of 0.9989. The calculation of the coefficient of determination can be found in Appendix E. The calibration curve along with the calibration data points for increasing power are plotted together in Figure 3. The data points for decreasing power are also plotted in Figure 1 in order to demonstrate the effects of hysteresis. The calibration voltage uncertainty and the

calibration pressure uncertainty, as seen in Table 1, are shown in Figure 3 as vertical and horizontal error bars, respectively.

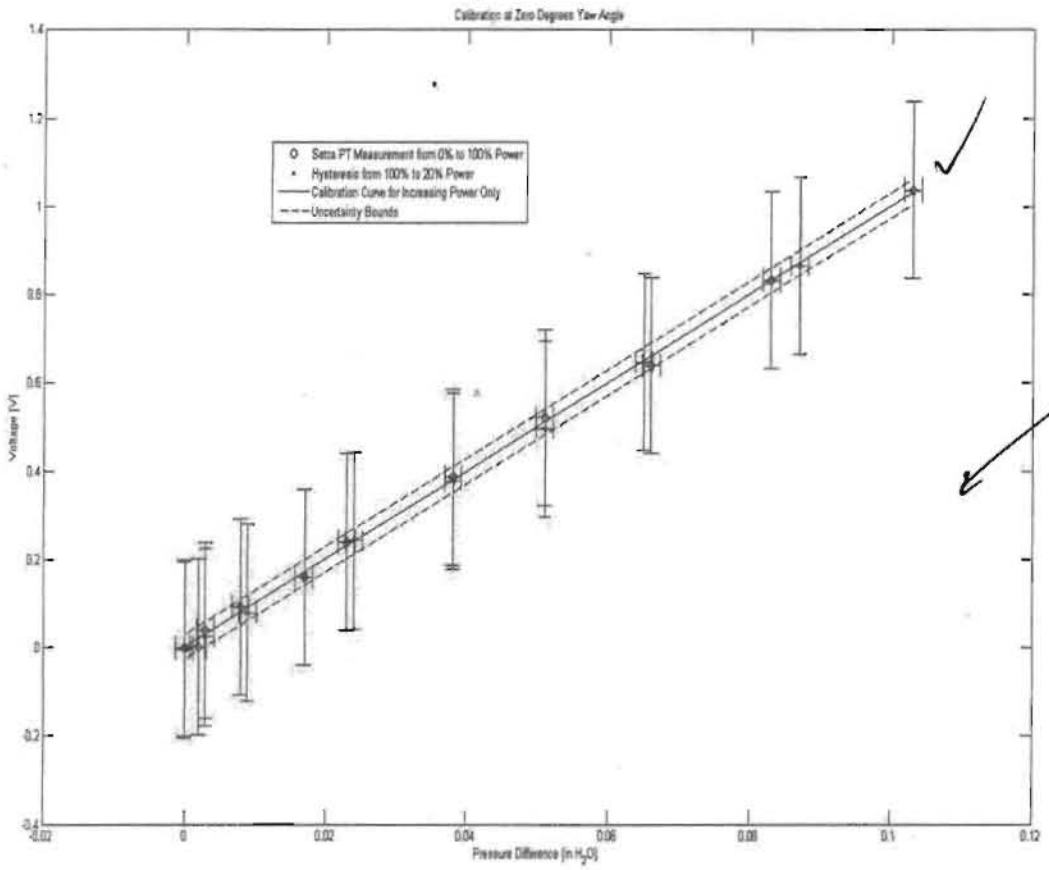

careful when copying matlab figures into a report often they end up having poor resolution

Figure 3: Calibration Curve, Calibration Data Points, and Hysteresis

Table 2 lists initial parameters found prior to the hand dryer measurements were completed. The Learning Center (LC) initial temperature and the barometric pressure were found from the thermometer and the barometer attached to the LC wind tunnel. From the initial temperature, the thermocouple was calibrated and was used to measure the temperature of the hand dryer flow. When this flow was found, it was used in equation [2] along with the barometric pressure to calculate the density of the fluid. The viscosity was also calculated to be $4.222*10^{-7}$ slug/ft-s and was combined with density in equation [1] to determine the actual characteristic length[13].

Table 2: Initial Measured and Calculated Parameters

Parameter	Value	Units	Measured or Calculated	Estimated Uncertainty (95% Confidence)
LC Initial Temperature	532.5	°R	Measured	± 0.09 °R
Barometric Pressure	29.52	in Hg	Measured	± 0.71 lb/ft^2
Hand Dryer Temperature	597	°R	Measured	± 13 °R
Density	0.002	slug/ft^3	Calculated	± 4.6*10^{-5} slug/ft^3
Actual Characteristic Length	4.541	in	Calculated	± 0.0017 in

4.2 Yaw Angle

The effect of yaw angle was studied using calibration data from kit 5. The voltage was sampled with the Setra PT for yaw angles of 0, 5, 10, 15, and 30 degrees. To show the yaw angle effect, the output voltage of the Setra PT for 100% wind tunnel power was plotted against yaw angle in Figure 4 (See Appendix C: MATLAB code). Table 3 compares the Setra PT voltage at yaw angle against the Setra PT voltage at zero yaw angle.

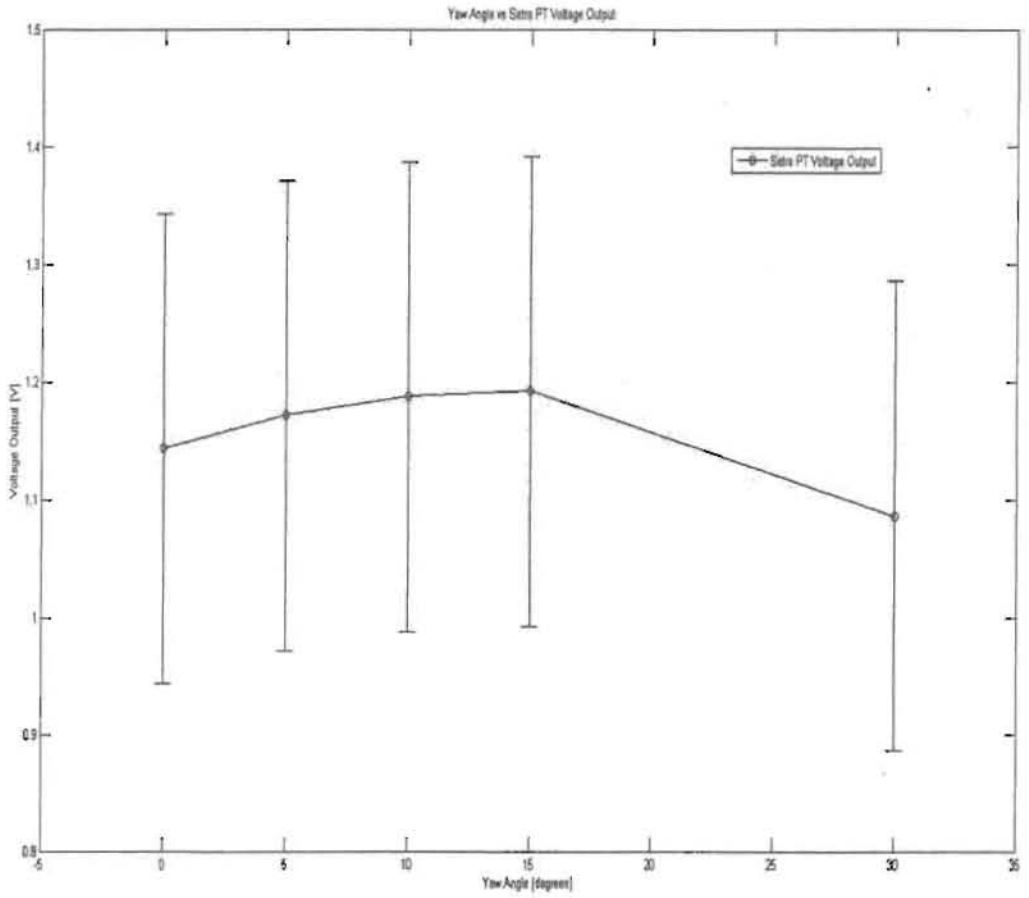

Figure 4: Setra PT Voltage for 100% Wind Tunnel Power vs Yaw Angle

Table 3: Percent Deviation of Setra PT Voltage Output for Yaw Angles

Yaw Angle (degrees)	Percent Deviation (%)
5	2.79
10	4.42
15	4.87
30	5.71

4.3 Velocity Profile of Xlerator Outlet and Flow Rate Results

Using the calculated calibration curve, and the Bernoulli equation, the velocity of the flow at the hand dryer outlet was determined for multiple points on an 8x8 grid mapping half of the Xlerator outlet. This calculated distribution was reflected across the center line at y = ½ inch (See Appendix B: MATLAB code). The resulting velocity profile of the Xlerator flow is shown in Figure 5.

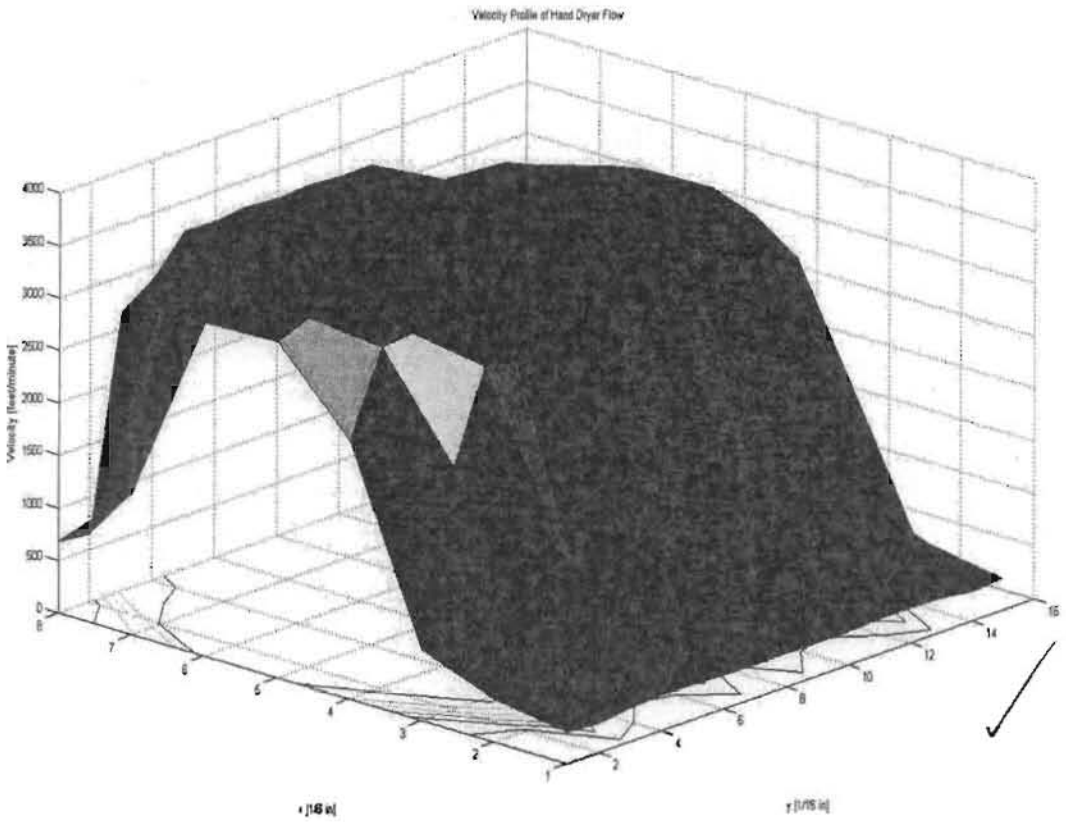

Figure 5: Velocity Flow Field of Xlerator Outlet

The volumetric flow rate of the hand dryer flow can be calculated using equation [5] (Table 4). Since a Cartesian coordinate grid was used to map the flow, the Simpson's Rule for integration (Equation [7]) was used to approximate the volumetric flow. This method was also used to approximate the mass flow rate; equation [8]. The mean velocity was then calculated by dividing the volumetric flow rate approximation by the area of the grid. (Equation [9]).

Table 4: Flow Rate and Velocity Results

Parameter	Value	Units	Measured or Calculated	Estimated Uncertainty (95% Confidence)
Volumetric Flow Rate	12.78	ft^3/min	Calculated	± 0.10 ft^3/min
Mass Flow Rate	0.026	slug/min	Calculated	± 0.070 slug/min
Mean Velocity	3,284	ft/min	Calculated	± 3.6 ft/min

4.4 Quantitative Comparison of Measured to Theoretical Data

After obtaining parameters for the actual flow of the Xlerator hand dryer, they were compared to the theoretical values and the manufacturer specifications. The Quantitative comparison of the actual values to theoretical values is presented in Table 5.

Table 5: Comparison of Measured to Theoretical Values

Parameter	Units	Actual	Theoretical	Percent Difference
Characteristic Length	in	4.541	0.926	390.4%
Mean Velocity	ft/min	3393	16000	78.8%
Hand Dryer Flow Temp.	°R	597	595	0.3%

5 Discussion

5.1 Evaluation and Analysis

In order to complete this field test, many assumptions had to be made. When the calibration curve was created, it was apparent that the range of the calibration was not sufficient to cover the range of hand dryer voltages (Figure 3). Since this was the case, the calibration curve was extrapolated to cover the values of the hand dryer. This assumption was practical because pitot static measurement systems are known to be linear over a large range of flows. The calibration curve coefficient of determination was calculated as 0.9989. Since this value is greater than 0.90, the correlation of the calibration curve is significant and the fit is good.

In figure 3, the effect of hysteresis on the calibration was compared to the actual values for the measurement system. It was found that the deceleration of the flow had little effect on the data point and the largest uncertainty due to hysteresis was found to be only 0.0148 V. While obtaining hand dryer data, the flow pressure was only measured while the flow was at a steady stage; therefore, hysteresis was not a factor in the hand dryer measurements.

In figure 4, the effect of yaw angle on the pitot static measurement system data was analyzed. From the graph, it can be seen that the voltage increases initially and then falls rapidly

as the yaw angle decreases. The effect of yaw angle on a pitot probe causes a larger pressure on the static pressure tap. This increase in pressure equalizes the displacement of the static pressure plenum and total pressure plenum causing the voltage to drop. This is why there should not be an increase in voltage, but this voltage drop can be attributed to the large amount of uncertainty in the measurements shown by the error bars in the figure. In table 3, the percent deviation of the yaw angle voltage reading compared to the initial voltage reading were calculated. From these values, it can be shown that the percent deviation increases as the angle increases.

Bernoulli's equation requires a number of assumptions that must be satisfied for the equation to be applied to the hand dryer flow. To ensure that the flow was laminar, the characteristic length of the hand dryer was calculated according to equation [1] before the flow was measured using the manufacturer's technical specifications (Table 2). Once this theoretical characteristic length was found, the pitot tube was placed well within the laminar section to guarantee that the flow would be laminar. After the true velocity of the hand dryer was found, the characteristic length was recalculated to confirm that the pitot tube was within the laminar flow. Since the pitot tube measurements were indeed taken in the laminar flow region, this proves that the Bernoulli equation assumption that the flow is along a streamline is valid. The assumption of inviscid flow can be proven because the Reynolds number is high. This indicates that the inertial forces are much greater than the viscous forces proving that the viscosity can be neglected altogether. Using the calculated mean velocity listed in table 4, the Mach number was calculated to be 0.05 (See Appendix F). This confirmed that the flow was incompressible because the Mach number value was less than 0.3. Because all of these assumptions were verified, it can be concluded that Bernoulli's equation can be applied to the hand dryer flow.

Once Bernoulli's equation, equation [4], was applied to the pressure distribution of the flow field, the velocity at each point was calculated. Figure 5, illustrates the velocity flow field of the Xlerator for the grid shown in Appendix A Figure 1. By taking advantage of the symmetry of pipe flow, the velocity distribution over the whole cross sectional area could be modeled by reflecting the graph at $y = ½$. Instead of the largest velocity appearing at the center of the outlet as expected, the largest velocity was measured near the wall. One possible explanation is that the blower in the hand dryer may not introduce a symmetrical velocity distribution. Another explanation is that there may be a pipe element upstream of the outlet that is affecting the shape of the flow. The outlet of the hand dryer is at an angle compared to the underside of the hand dryer. So, unless that pipe angle is constant from the blower to the exit, the velocity distribution may be affected by a bend in the pipe. If this is the case, the calculated mean velocity, volumetric flow rate, and mass flow rate will be underestimated (Table 4).

Even though the mean velocity may be underestimated, it is only ¼ of the manufacturer's specified velocity. Although it may be convenient to assume that the hand dryer is underperforming because of overuse or mechanical failure, it is more likely that the hand dryer was installed to perform at a lower speed. Xlerator production began in 2002 and has a full warranty for 5 years. Unless the 2nd floor LaFortune Xlerator was installed before 2004, it should be in full working order. The more likely explanation is that the Xlerator was intended to produce a reduced velocity. This could be accomplished if either the Xlerator was installed with a different blower operating mode or the voltage sent to the Xlerator is reduced. Even though reducing the voltage sent to the Xlerator is a possible explanation, a comparison of the measured flow temperature and the technical specification's temperature four inches below the outlet proves that this explanation is invalid. When these two temperatures are compared in figure 5, they only differ by 0.3%. If the voltage of the Xlerator was reduced, this would also reduce the temperature of the flow.

Not necessarily, heating elements are often high current / high resistance devices (low voltage)

5.2 Improvements

If this experiment was repeated there are some improvements that can be made to the experimental approach. To reduce the uncertainty of the measurements, a more accurate portable pressure transducer should be utilized. The instrument uncertainty should be less than 0.1% of the full scale range to sufficiently reduce the error. Also, the accuracy of the conversion from the pressure transducer to voltage should be increase by obtaining calibration data for the full range of pressure differences. This would eliminate the error associated with extrapolating the calibration curve.

The experimental setup could be improved with a more accurate grid system and an improved grid. Instead of placing the pitot tube on cardboard and recycling bins and measuring the distance with paper rulers, a grid should be built as a stand with metal bars that have notches at each measuring point. Then the pitot tube will be locked into each position that will be accurately measured. The angle that the pitot tube makes with the outlet should also be measured using a protractors so that yaw angle does not effect the measurements. A new grid should be developed that covers the entire cross-sectional area of the outlet so that the error associated with symmetry assumptions can be negated. Finally, the grid should be converted to a polar coordinate system originating at the center of the pipe. The polar coordinate system would improve the representation of the velocity flow field contour.

6 Conclusions

In conclusion, the flow analysis of the XL-W Xlerator hand dryer in the LaFortune second floor men's bathroom determined the actual mean velocity of the output to be 3,284 ± 3.6 ft/min (95%) which was 78.8% less than the velocity listed in the manufacturer specifications. Possible reasons for this large of a discrepancy between the measured and theoretical velocity values are overuse, mechanical failure, or a reduction of voltage, but the most feasible reason was concluded to be that the hand dryer was running at a lower operational power setting. The hand dryer flow temperature was measured to be 597 ± 13 °R (95%) which is only 0.3% different than the listed manufacturer specifications. This supports the conclusion that the hand dryer was operating at a lower operational power setting. The flow analysis also determined that the actual volumetric flow rate was 12.78 ± 0.10 ft^3/min (95%) and the actual mass flow rate to be 0.026 ± 0.070 slug/min (95%). Analysis of the uncertainty of hysteresis found that hysteresis had no effect on the hand dryer measurements from the pitot static measurement system. An investigation into the effect of yaw angle on the pitot static measurement system concluded that as yaw angle increased, the pressure difference measured by the pitot probe decreased. However, it was found that yaw angles of less than 5 degrees produced little effect.

Great report!

7 References

[1] "Xlerator- Surface Mounted – Hand Dryers," Excel Dryer, Inc., East Longmeadow, MA, http://www.nd.edu/%7Epbowles/ame20213/handdryer.pdf
[2] 2009, "Lab Exercise #4: Practical Experiments", AME 20213. University of Notre Dame.
[3] Bowles, P., 2009, "LEX-4: Introduction to the Bernoulli Equation," AME 20213. University of Notre Dame. http://www.nd.edu/%7Epbowles/ame20213/Intro.pdf
[4] Bowles, P., 2009, "2-D Numerical Integration of Experimental Data," AME 20213. University of Notre Dame. http://www.nd.edu/%7Epbowles/ame20213/integration.pdf
[5] "Multi-Sense Series- Model 260 Specifications," Setra, Boxborough, MA, http://www.nd.edu/%7Epbowles/ame20213/specs_260B.pdf
[6] "Model 239/C239 Specifications," Setra, Boxbourough, MA, http://www.nd.edu/%7Epbowles/ame20213/specs_239.pdf
[7] Go, D., 2009, "Introduction to Measurements and Data Analysis Lecture Notes," AME 20213. University of Notre Dame.
[8] "Thermocouple Tolerances," Omega Engineering, Inc., Stamford, CT, http://www.nd.edu/%7Epbowles/ame20213/thermocouple.pdf
[9] "Monolithic Thermocouple Amplifiers with Cold Junction Compenstation," Analog Devices, Norwood, MA, http://www.nd.edu/%7Epbowles/ame20213/AD595.pdf
[10] Dunn, P., 2009, "Measurements and Mechanical Engineering," University of Notre Dame. All equations, unless otherwise noted, come from lab handout:
[11] 2009, "Lab Exercise #3: Sampling Unsteady Physical Stimulus", AME 20213. University of Notre Dame.
[12] 2005, "Air – Temperature, Pressure, and Density," The Engineering ToolBox, http://www.engineeringtoolbox.com/air-temperature-pressure-density-d_771.html
[13] 2005, "Air- Absolute and Kinematic Viscosity," The Engineering ToolBox, http://www.engineeringtoolbox.com/air-absolute-kinematic-viscosity-d_601.html
[14] 2009, "GPS as Pitot Tube Backup?" Airliners.net. http://www.airliners.net/aviation-forums/tech_ops/read.main/256215/1/

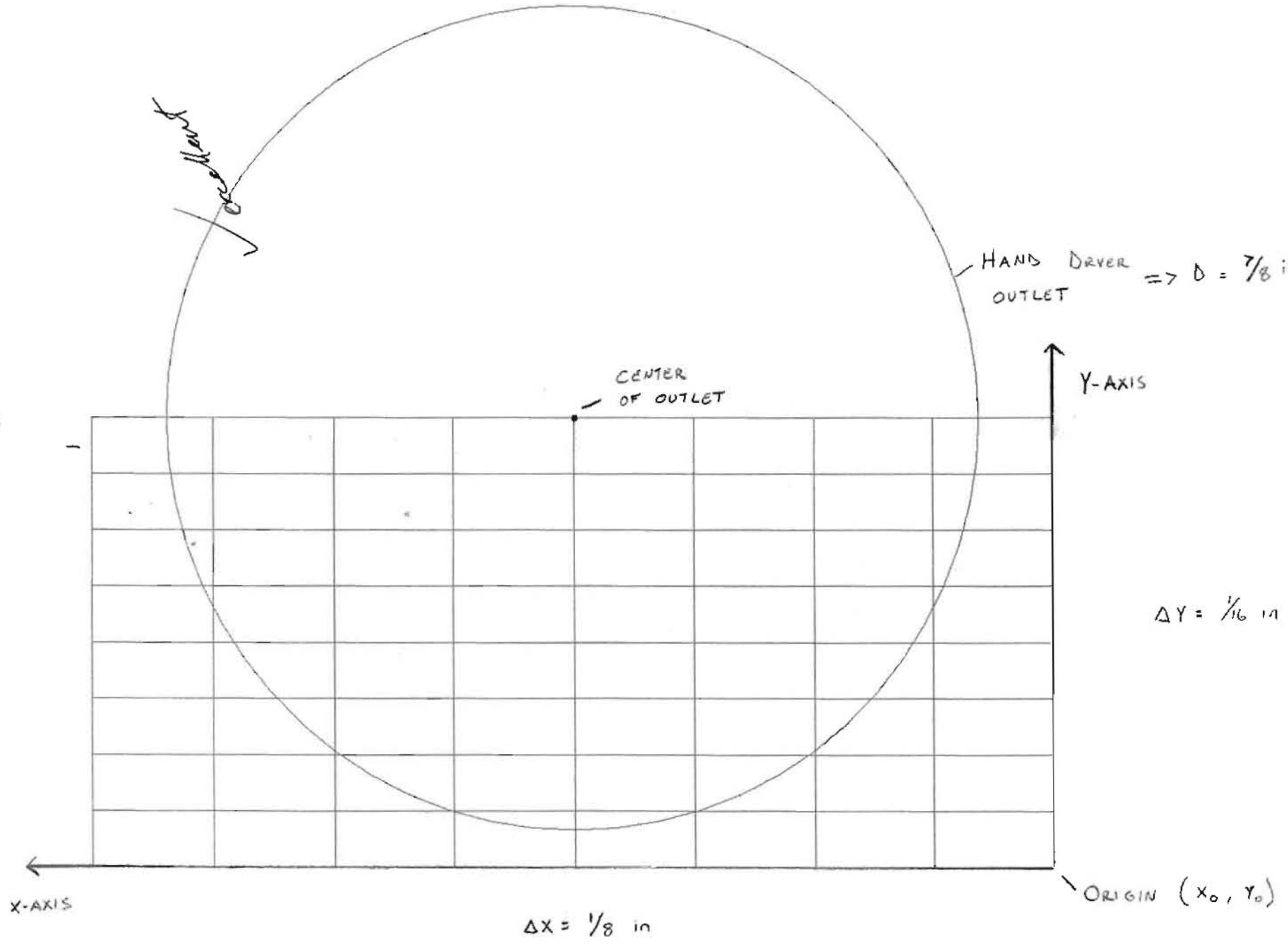

Appendix A - Figure 1